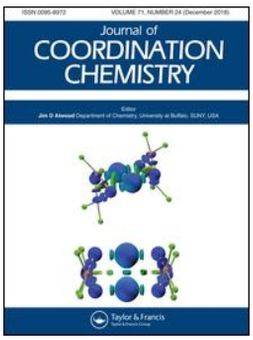

Journal of Coordination Chemistry

ISSN: 0095-8972 (Print) 1029-0389 (Online) Journal homepage: https://www.tandfonline.com/loi/gcoo20

Design, structural, C–H....H–C supramolecular interactions and computational investigations of $Cd(N\cap N'')X_2$ complexes based on an asymmetrical 1,2-diamine ligand: physicochemical and thermal analysis

Ismail Warad, Khaled Alkanad, Mohammed Suleiman, Karthik Kumara, Anas Al-Ali, Yasser H. E. Mohammed, Neartur K. Lokanath & Abdelkader Zarrouk

To cite this article: Ismail Warad, Khaled Alkanad, Mohammed Suleiman, Karthik Kumara, Anas Al-Ali, Yasser H. E. Mohammed, Neartur K. Lokanath & Abdelkader Zarrouk (2019): Design, structural, C–H….H–C supramolecular interactions and computational investigations of $Cd(N\cap N'')X_2$ complexes based on an asymmetrical 1,2-diamine ligand: physicochemical and thermal analysis, Journal of Coordination Chemistry, DOI: 10.1080/00958972.2019.1696960

To link to this article: https://doi.org/10.1080/00958972.2019.1696960

Published online: 02 Dec 2019.

JOURNAL OF COORDINATION CHEMISTRY
https://doi.org/10.1080/00958972.2019.1696960

Taylor & Francis
Taylor & Francis Group

Design, structural, C–H … .H–C supramolecular interactions and computational investigations of $Cd(N\cap N'')X_2$ complexes based on an asymmetrical 1,2-diamine ligand: physicochemical and thermal analysis

Ismail Warad[a,b], Khaled Alkanad[c], Mohammed Suleiman[b], Karthik Kumara[b], Anas Al-Ali[a], Yasser H. E. Mohammed[d], Neartur K. Lokanath[b] and Abdelkader Zarrouk[e]

[a]Department of Chemistry and Earth Sciences, Qatar University, Doha, Qatar; [b]Department of Chemistry, Science College, An-Najah National University, Nablus, Palestine; [c]Department of Studies in Physics, University of Mysore, Manasagangotri, Mysore, India; [d]Department of Biochemistry, Faculty of Applied Science College, University of Hajjah, Yemen; [e]Laboratory of Materials, Nanotechnology and Environment, Mohammed V University, Faculty of Sciences, Rabat, Morocco

ABSTRACT

Complexes $[N\cap N''CdX_2]$ (X = Cl (**1**), I (**2**) and $N\cap N''$ is N1,N1,N2-triethylethane-1,2-diamine) are reported. The desired complexes were prepared under identical synthetic conditions and characterized by ESI-MS, UV-vis, CHN-elemental analyses, ^{1}H-NMR and FT-IR. The structure of **2** has been confirmed by XRD studies, wherein $N\cap N''CdI_2$ complex crystallized in the monoclinic space group $P2_1/n$ with $a = 9.245(8)$ Å, $b = 15.190(12)$ Å, $c = 10.905(9)$ Å, $V = 1491(2)$ Å^3, and $Z = 4$. Distorted tetrahedral geometry around the Cd(II), constructed from 2N and 2I, was confirmed by single crystal XRD. Only C–H … .H–C supramolecular interactions have been detected in **2**. Hirshfeld surface analysis (HSA) reflected presence of weak H … .H noncovalent supramolecular interactions and presence of no H … .I bonds are consistent with the experimental XRD-result. Mulliken population charge and molecular electrostatic potential (MEP) calculations for $N\cap N''CdI_2$ were carried out to support the XRD-result. The computed electronic parameters B3LYP-IR, frontier molecular orbital (FMO), time-dependent self-consistent field/density functional theory (TD-SCF/DFT), and the global reactivity descriptors (GRD) quantum numbers were estimated and compared to the experimental data. Thermal stability studies of the $N\cap N''CdI_2$ complex were carried out *via* TGA/DTG from 0 to 800 °C in open atmosphere.

ARTICLE HISTORY
Received 6 February 2019
Accepted 4 November 2019

KEYWORDS
Cd(II) complex; DFT; XRD; HAS; TG/DTG

CONTACT Ismail Warad Ismail.warad@qu.edu.qa; warad@najah.edu Department of Chemistry and Earth Sciences, Qatar University, Doha, Qatar

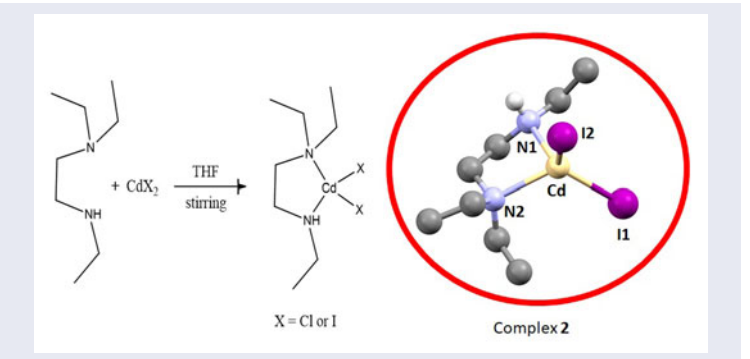

1. Introduction

In cadmium(II) complexes, several coordination modes are observed with octahedral to tetrahedral geometries expected [1–5]. Cadmium(II) coordination complexes usually exhibit good transparency in the UV-region [6–10], being colorless [10].

Among poly-chelate donor ligands, diamines have excellent coordination with metal ions including Cd(II) [11]. Extensive work has been performed in preparation and characterization of several types of Cd(II) complexes which coordinated to chelate ligands including diamines with the structure confirmed by XRD [3–12]. These complexes opened up a new procedure to synthesize CdO nanoparticles *via* thermal decomposition under mild, open atmosphere conditions [6, 8, 12–14].

Several Cd(II)/diamine complexes have been synthesized for solid state, biological and catalysis studies; many mononuclear tetrahedral cadmium(II) diiodide complexes with diverse bidentate asymmetrical N,N-diamine ligands have been reported, especially their XRD-crystal structure measurements [7–17].

Simple tetrahedral complexes with N∩N″CdX_2 general formula were prepared in this study, the N∩N″CdI_2 structure has been obtained by XRD and computed by HSA and DFT to rationalize the H … H noncovalent supramolecular intermolecular forces obtained *via* XRD, HSA, MPE, and Mull have been computed to be compared to XRD-packing result. The experimental-XRD/calculated-DFT-structure parameters like angles and bond lengths were also matched. The TD-SCF/DFT together with B3LYP-IR, FMO, and GRD quantum parameters were performed. The thermal behavior of N∩N″CdI_2 has been studied *via* TG/DTG.

2. Experimental

2.1. X-ray diffraction

A colorless block crystal of [N∩N″CdI_2] with the dimension of $0.32 \times 0.27 \times 0.25$ mm was used for XRD analysis; the XRD data are provided in Table 1.

2.2. Physical and computational measurements

CHN-analysis was carried out on an EL Elementar-Vario analyzer. IR spectroscopy was performed using a Perkin–Elmer 621 from 500 to 4000 cm^{-1}. Pharmacia LKB-Biochrom

Table 1. Crystal data, experimental and final refinement results for N∩N″CdI_2.

CCDC	1860218
Temperature	293(2)
Formula	$C_8H_{20}CdI_2N_2$
Molecular weight	510.46
Density	2.274 mg m^{-3}
Wavelength	0.71073 nm
Crystal system, space group	Monoclinic, P 21/n
Volume	1491(2) Å
Unit cell	
a	9.245(8) Å
b	15.190(12) Å
c	10.905(9) Å
Β	103.185(9)°
No. of measured, independent and observed [I > 2σ(*I*)] reflections	3614, 2318, 1979
Rint	0.12
R[F2 > 2σ(F2)], wR(F2), S	0.071, 0.165, 1.02
Δρmax, Δρmin (e $Å^{-3}$)	2.41, −2.79
Crystal size	0.32 × 0.27 × 0.25 mm
Z	4
Absorption correction	"Multi-scan"
Absorption coefficient	5.576 mu
F000	944.0
θ_{max}, θ_{min}	24.4°, 3.3°
T_{min}, T_{max}	0.183, 0.248

4060 served to measure UV-vis absorption spectra. The EDX was performed on a JSM-6360. NMR spectra were obtained using $CDCl_3$ on a DRX 250 Bruker-spectrometer. XRD data were collected on a Rigaku XtaLAB mini CCD diffractometer using Mo-Kα radiation of wavelength 0.71073 Å. The structure was solved using *SHELXS* and refined with *SHELXL* programs [18]. The DFT-computations were carried out in gaseous phase using Gaussian09 software at B3LYP/DFT with 6-311 G(d,p) basis set for all the light atoms (C, N, and H); for Cd and I their potential effective core LANL2DZ was performed [19]. CRYSTAL EXPLORER 3.1 program was used for HSA evaluation [20].

2.3. Synthesis of complexes

A THF solution (20 mL) of CdX_2 (1 mmol, 0.18 g from $CdCl_2$ or 0.37 g from CdI_2) was mixed individually with (1.1 mmol, 0.16 g) of N1,N1,N2-triethylethane-1,2-diamine dissolved in 10 mL THF. The mixture was stirred until a white precipitate formed (10–20 min), then filtered off, the filtrate was washed well with 80 mL of *n*-hexane and diethyl ether. Crystals suitable for XRD-diffraction studies were collected *via* evaporation of [EtOH:CH_2Cl_2] solvents from N∩N″CdI_2 diluted solution mixture.

Complex **1**: Yield: 0.257 g (78%), Colorless, m.p. 360 °C; ^{1}H NMR ($CDCl_3$, ppm) 1.08 (m, 9 H, $3CH_3$), 2.72 (m, 6 H, $3C\underline{H_2}CH_3$), 2.92 (m, 4 H, NCH_2CH_2N), IR ν (cm^{-1}) = 3328 (s, N-H), 2970–2780 (m, C-H), 1580 (w, N-H_{bend}), 1460 (s, C-H_{bend}), 1275 (w, C-N), 1124 (w, C-C), 505 (m, Cd-N). UV-Vis: λ_{max} (MeOH) 240 nm.

Complex **2**: Yield: 0.420 g (82%), Colorless, m.p. 240 °C; ^{1}H NMR ($CDCl_3$, ppm) 1.02 (m, 9 H, $3CH_3$), 2.68 (m, 6 H, $3C\underline{H_2}CH_3$), 2.86 (m, 4 H, NCH_2CH_2N), IR ν (cm^{-1}) = 3323

(s, N-H), 2950–2750 (m, C-H), 1590 (w, N-H_{bend}), (s, C-H_{bend}), 1265 (w, C-N), 1120 (w, C-C), 502 (m, Cd-N). UV-Vis: λ_{max} (MeOH) 245 nm.

3. Results and discussion

3.1. Synthesis, MS, EA, and EDX

Direct mixing of equivalent amounts of CdX_2 (X = Cl and I) dissolved in THF with an equivalent amount of the N1,N1,N2-triethylethane-1,2-diamine as a bidentate asymmetrical ligand dissolved also in THF afforded the desired tetrahedral complexes [N∩N″$CdCl_2$] (**1**) and [N∩N″CdI_2] (**2**) (Scheme 1). The N,NCdI_2 structure has been proven by XRD measurement; the complexes are soluble in chlorinated solvents, CH_2Cl_2 and $CHCl_3$. The complexes insoluble in nonpolar ethers and *n*-hexane or highly polar solvents like water. The spectral and analytical analyses are consistent with the proposed formulas.

ESI-MS (*m/z*) of [N∩N″$CdCl_2$] reflected a charged ion at 328.10 [M] from [$C_8H_{20}CdCl_2N_2$], 327.6 (theoretical). CHN-analysis; Calcd: C, 29.33; H, 6.15; N, 8.55. Found: C, 29.19; H, 6.08; N, 8.48%. MS (*m/z*) of [N∩N″CdI_2] reflected a charged ion at 511.8 [M] (Figure 1) from [$C_8H_{20}CdI_2N_2$], 510.5 (theoretical). CHN-analysis; Calcd: C, 18.82; H, 3.95; N, 5.49%. Found: C, 18.75; H, 3.87; N, 5.52%.

EDX analysis reflected the presence of four types of atoms corresponding to the complexes content C, N, X, and Cd elements, for example, **1** EDX reflected the presence of Cl, C, N, and Cd only, as seen in Figure 2(a), while **2** EDX reflected the presence of I, C, N, and Cd, as seen in Figure 2(b). CHN-elemental analysis, EDX and MS data are consistent with [N∩N″CdX_2].

3.2. XRD and DFT comparison

In **2** slightly distorted tetrahedral (Td) coordination around Cd(II) was detected *via* XRD then supported by DFT analysis as seen in Figure 3(a). The XRD distances around Cd(II) are Cd-I1 2.690 Å, Cd-I2 2.724 Å, Cd-N1 2.299 Å, and Cd-N2 2.341 Å; the angles were I1-Cd-I2 123.5(°), I1-Cd1-N1 115.1(°), I1-Cd1-N1 109.9(°), and N1-Cd1-N2 79.7(°) (Table 2). The complex crystallized in the monoclinic system with $P2_1/n$ space group and Z = 4, as in Figure 3(b). The Td geometry of Cd(II) is consistent with similar complexes [7–17], moreover, the Cd-I and Cd-N bond distances and N-Cd-N and I-Cd-I bond angles fall within the typical ranges of similar systems [7–17]. Even in the presence of H atoms as electrophiles and I/N atoms as nucleophiles, no H-bonds were detected compared to other similar systems [8–12]. In the crystal lattice, only one

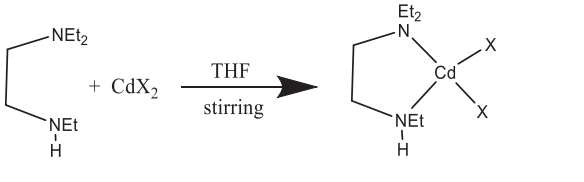

X = Cl (Complex **1**) or I (Complex **2**)

Scheme 1. Synthesis of the complexes.

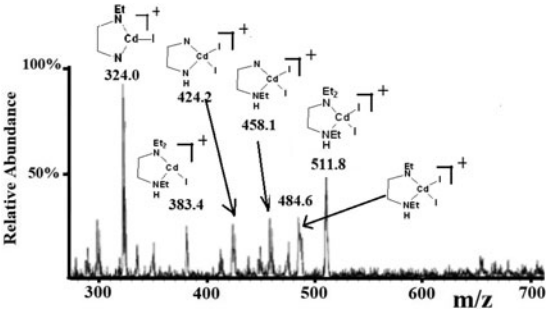

Figure 1. ESI-MS of [N∩N″CdI_2].

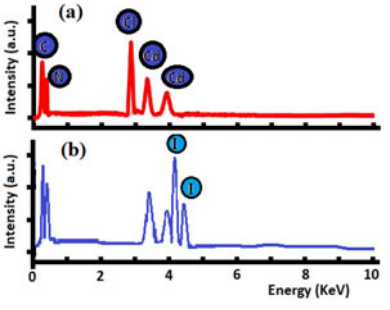

Figure 2. EDX of (a) [N∩N″$CdCl_2$] and (b) [N∩N″CdI_2].

weak C–H….H–C supramolecular interaction was detected, consistent with recent data [16]; no other significant interactions such as halogen-centroid, π…π, H…π, or H-bond were detected (Figure 3(c). In **2** self-assembly by weak and reversible H….H noncovalent supramolecular interactions with 2.206 Å chained the structure to a polynuclear 1D network. The DFT/B3LYP-optimized parameters of the N∩N″CdI_2 structure (angles and bond lengths) were compared to the experimental XRD, as shown in Table 2 and Figure 4.

Agreement between XRD and DFT results in bond lengths with $R^2 = 0.996$ (Figure 4(a,b)) and in angles with $R^2 = 0.909$ (Figure 4(c,d)) were observed. Generality of the DFT and XRD structure parameters matched [12].

3.3. FT-IR

The complexation reaction was observed by IR in order to evaluate the CdI_2 and N1,N1,N2-triethylethane-1,2-diamine IR behavior before and after their coordination to prepare the desired N∩N″CdI_2 complex, as seen in Figure 5(a–c). Moreover, DFT-IR of N∩N″CdI_2 has been computed in order to determine the degree of compatibility between the experimental and B3LYP-IR data, as seen in Figure 5(d,e). The preparation of N∩N″CdI_2 can be supported mainly by the N–H vibration shifting from 3363 cm^{-1} (N∩N″free ligand, Figure 5(b)) to 3323 cm^{-1} (N∩N″CdI_2, Figure 5(c)) with $\Delta\upsilon = 40\,cm^{-1}$ and the appearance of a new signal at 502 cm^{-1} from the Cd-N coordination bond (Figure 5(c)). All the other functional groups are in their expected vibrational positions

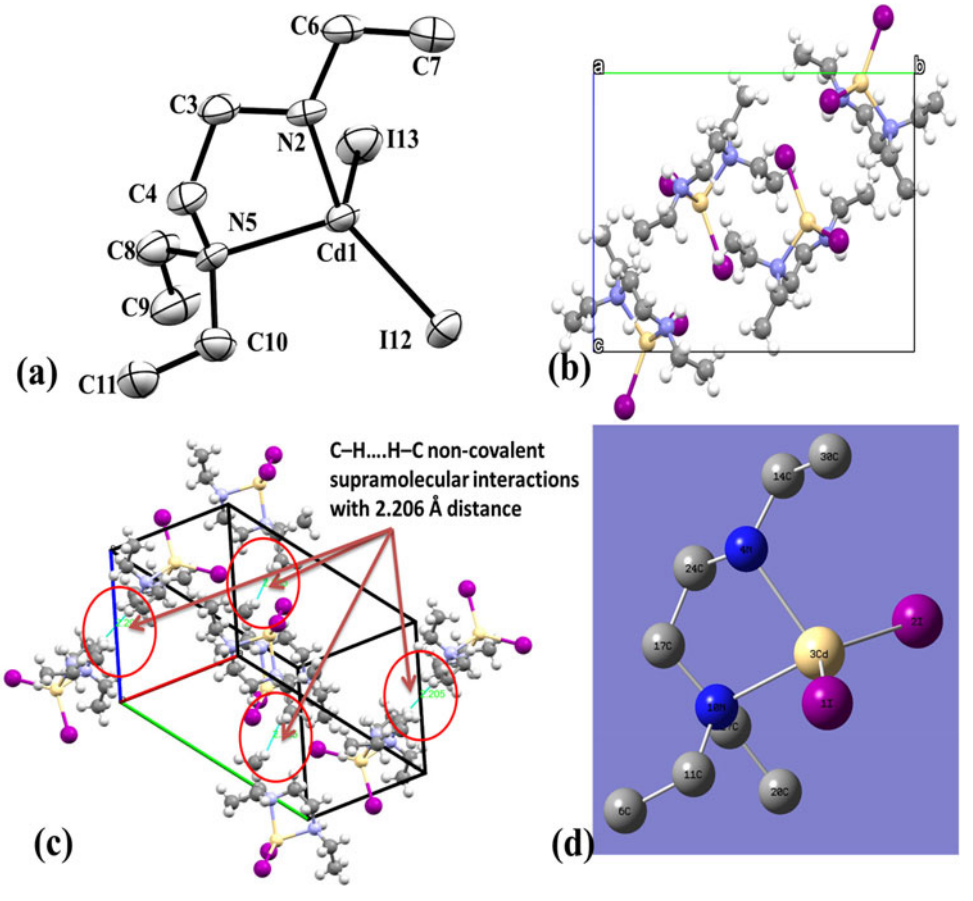

Figure 3. View of **2**: (a) ORTEP, (b) 2D-packing unit cell along the *a*-axis, (c) 3D-packing unit cell with $Z = 4$ and 4C-H … H-C interactions and (d) DFT-optimized structure.

Table 2. XRD-Exp./DFT-structure parameters of [N∩N˝$CdCl_2$].

Bond No.	Bonds (Å)	Exp. XRD	DFT	Angle No.	Angles (°)	Exp. XRD	DFT
1	I12-Cd1	2.690	2.824	1	I12-Cd1-I13	123.53	135.30
2	I13-Cd1	2.724	2.836	2	I12-Cd1-N2	115.10	107.78
3	Cd1-N2	2.299	2.399	3	I12-Cd1-N5	109.90	107.71
4	Cd1-N5	2.341	2.345	4	I13-Cd1-N2	105.70	109.42
5	N2-C6	1.500	1.511	5	I13-Cd1-N5	114.60	102.47
6	N2-C3	1.480	1.502	6	N2-Cd1-N5	79.70	79.82
7	C11-C10	1.500	1.540	7	Cd1-N2-C6	116.50	115.20
8	N5-C10	1.510	1.519	8	Cd1-N2-C3	104.80	102.99
9	N5-C4	1.480	1.511	9	C6-N2-C3	111.70	112.82
10	N5-C8	1.470	1.518	10	Cd1-N5-C10	107.20	109.91
11	C6-C7	1.530	1.534	11	Cd1-N5-C4	104.30	103.55
12	C4-C3	1.540	1.538	12	Cd1-N5-C8	112.70	110.40
13	C9-C8	1.480	1.535	13	C10-N5-C4	111.20	110.36
				14	C10-N5-C8	113.00	112.32
				15	C4-N5-C8	108.10	109.96
				16	C11-C10-N5	115.50	115.31
				17	N2-C6-C7	108.90	110.36
				18	N5-C4-C3	114.20	112.75
				19	N2-C3-C4	108.10	110.35

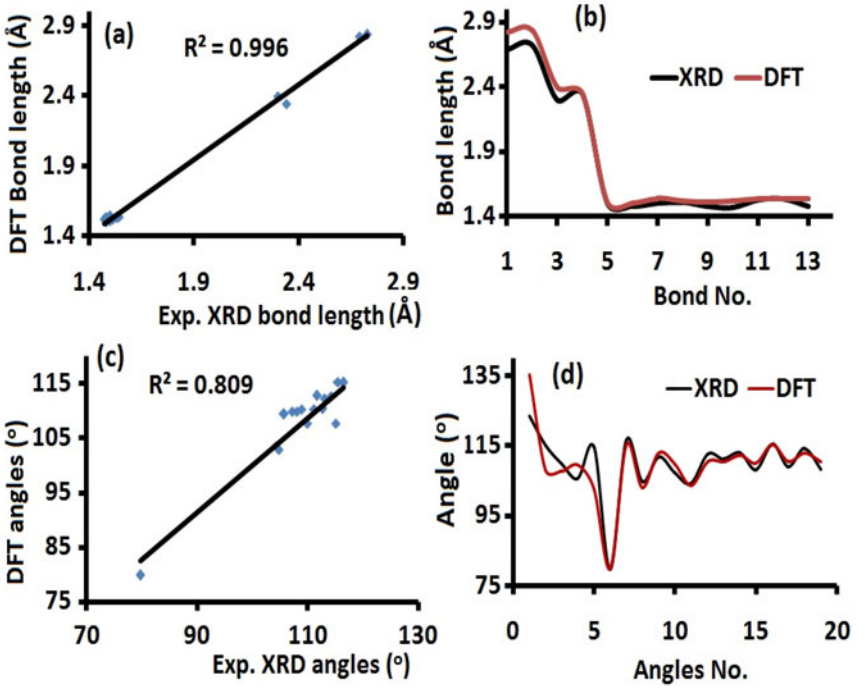

Figure 4. For N∩N″CdI_2: (a) XRD/DFT bond lengths graphical correlation, (b) diagram of XRD/DFT bond lengths, (c) XRD/DFT angles graphical correlation, and (d) diagram of XRD/DFT angles.

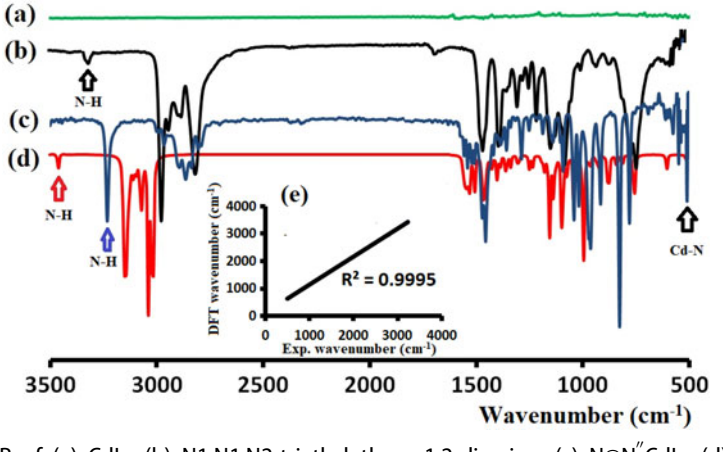

Figure 5. FT-IR of (a) CdI_2, (b) N1,N1,N2-triethylethane-1,2-diamine, (c) N∩N″CdI_2, (d) B3LYP-IR of N∩N″CdI_2, and (e) Exp./DFT-IR graphical correlation of N∩N″CdI_2.

[8, 12, 14]. Excellent agreement between DFT and experimental IR for N∩N″CdI_2 with $R^2 = 0.9995$ is shown in Figure 5(e).

3.4. HOMO-LUMO, TD-SCF-B3LYP, electronic transfer and GRD investigation

For N∩N″CdI_2, the HOMO/LUMO energy diagram and shapes are illustrated in Figure 6(a). The electron donation capacity $\Delta E_{HOMO/LUMO} = 5.4042$ eV (∼232.0 nm) reflected a

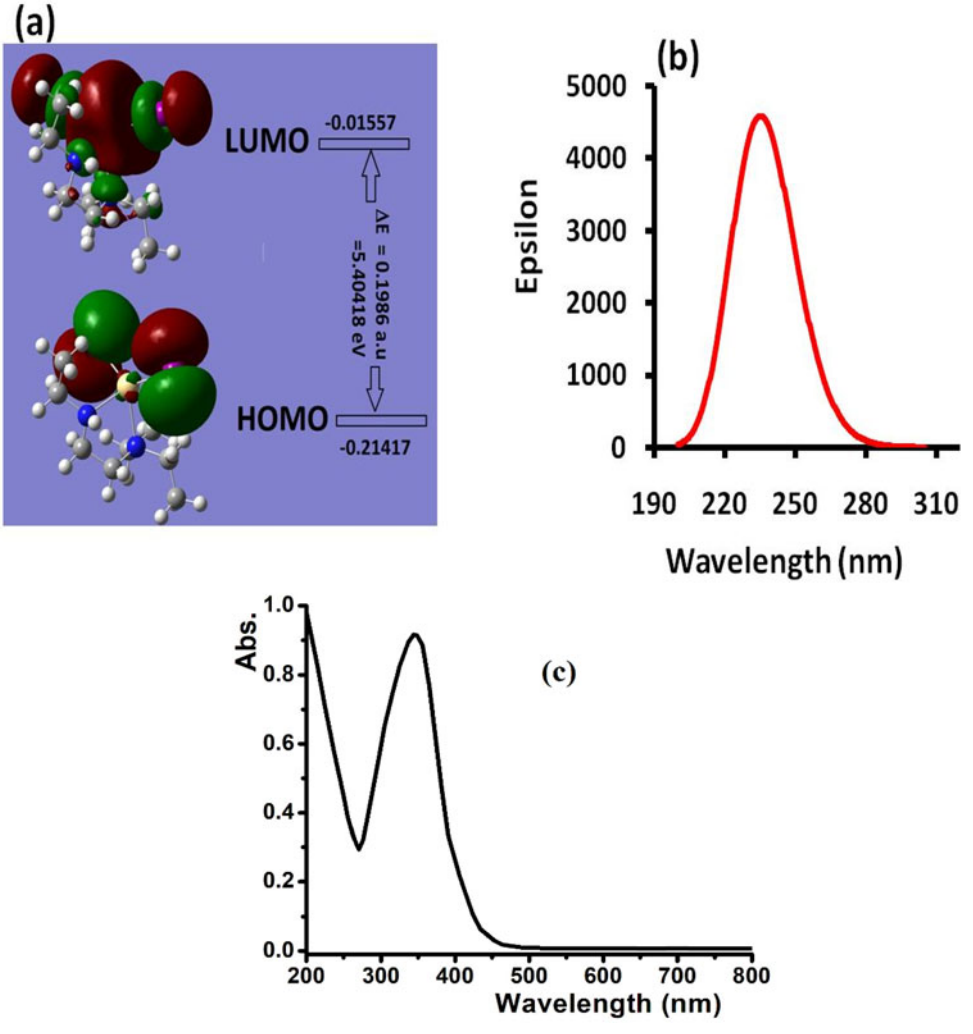

Figure 6. (a) HOMO/LUMO, (b) TD-SCF-calculated, and (c) experimental electronic spectra of N∩N″CdI_2 in methanol.

Table 3. TD-SCF Electronic parameters for N∩N″CdI_2.

No.	Energy (kJ/mol)	Wavelength (nm)	Osc. Strength	Major/Minor contribs	
1	496.52	240.931	0.0498	HOMO→LUMO (96%)	
2	502.74	237.949	0.0011	H-1→LUMO (95%)	H-1→L + 1 (2%)
3	516.98	231.394	0.0702	H-2→LUMO (94%)	H-2→L + 1 (3%)

sharp absorption in the ultraviolet region. The DFT/TD-SCF in methanol agrees with a broad absorption at 200–280 nm with overall $\lambda_{max} \sim 240$ nm corresponding mainly to HOMO/LUMO (96%) e-transition (Figure 6(b)). The other DFT e-transition together with the molecular-contribution ratios are illustrated in Table 3. Exp. spectrum of N∩N″CdI_2 in the same solvent (methanol) reflected a broad peak at $\lambda_{max} = 245$ nm, which was attributed to $\pi \rightarrow \pi^*$ e-transition. No MLCT or d to d transitions in the visible area were

Table 4. Calculated quantum parameters of N,NCdI$_2$.

GRD		Value
Global total energy	E_T	–497.37079722 a.u,
Low unoccupied molecular orbital	LUMO	–0.01557 a.u.
High occupied molecular orbital	HOMO	–0.21417 a.u.
Energy difference	ΔE_{gap}	0.1986 a.u. (5.40418 eV)
Electron affinity	A	0.42368 eV
Ionization potential	I	5.82786 eV
Global hardness		2.7024 eV
Global softness	σ	0.37004 eV
Chemical potential	μ	–3.12577 eV
Absolute electronegativity	X	3.12577 eV
Electrophilicity	ω	1.807733 eV
Dipole moment	ψ	9.6698 D

detected (Figure 6(c)). The TD-SCF transition (Figure 6(b)) is consistent with the collected experimental results (Figure 6(c)); perhaps the small shift in λ_{max} ($\Delta\lambda \sim 5$ nm) can be attributed to solute-solvent interactions [14].

GRD quantum parameters, electrophilicity (ω), the chemical potential (μ), softness (σ), hardness (), and electronegativity (χ), of the molecule were elaborated by using the following equations:

$$I : \text{Ionization potential} = -E_{HOMO} \quad (1)$$

$$\Α : \text{Electron affinity} = -E_{LUMO} \quad (2)$$

$$\Delta E_{gap} : \text{Energy gap} = E_{HOMO} - E_{LOMO} \quad (3)$$

$$\chi : \text{Absolute electronegativity} = \frac{I + \Α}{2} \quad (4)$$

$$\eta : \text{Global hardness} = \frac{I - \Α}{2} \quad (5)$$

$$\sigma : \text{Global softness} = \frac{1}{\eta} \quad (6)$$

$$\mu : \text{Chemical potential} = -\chi \quad (7)$$

$$\omega : \text{Electrophilicity} = \frac{\mu^2}{2\eta} \quad (8)$$

The GRD data values are collected in Table 4.

3.5. HSA, MEP, and Mulliken investigations

Theoretical HSA [21–27] estimations are devoted to analyzing the C–H … .H–C supramolecular noncovalent interactions. One red spot was detected approaching one of the terminal CH_3 hydrogens as in the d_{norm} surface reflecting the formation of H … H intermolecular interaction (Figure 7), consistent with the XRD collected data [22].

The 2D-Fingerprint plots over the HSA computed surface molecule reflected the appearance of contacts like H … H(58.4%)>H … I(12.5%)>H … Cd(0.4%)>H … N and H … C(0.0%) with (71.3%) H … overall connections, as depicted in Figure 7(d). The MEP proved the presence of both e-rich/e-poor positions on the complex surface (Figure 8), for example, iodides are nucleophile sites since it is reflected with the red color. On the other hand, the blue color of the ethylene H showed a strong electrophile, while

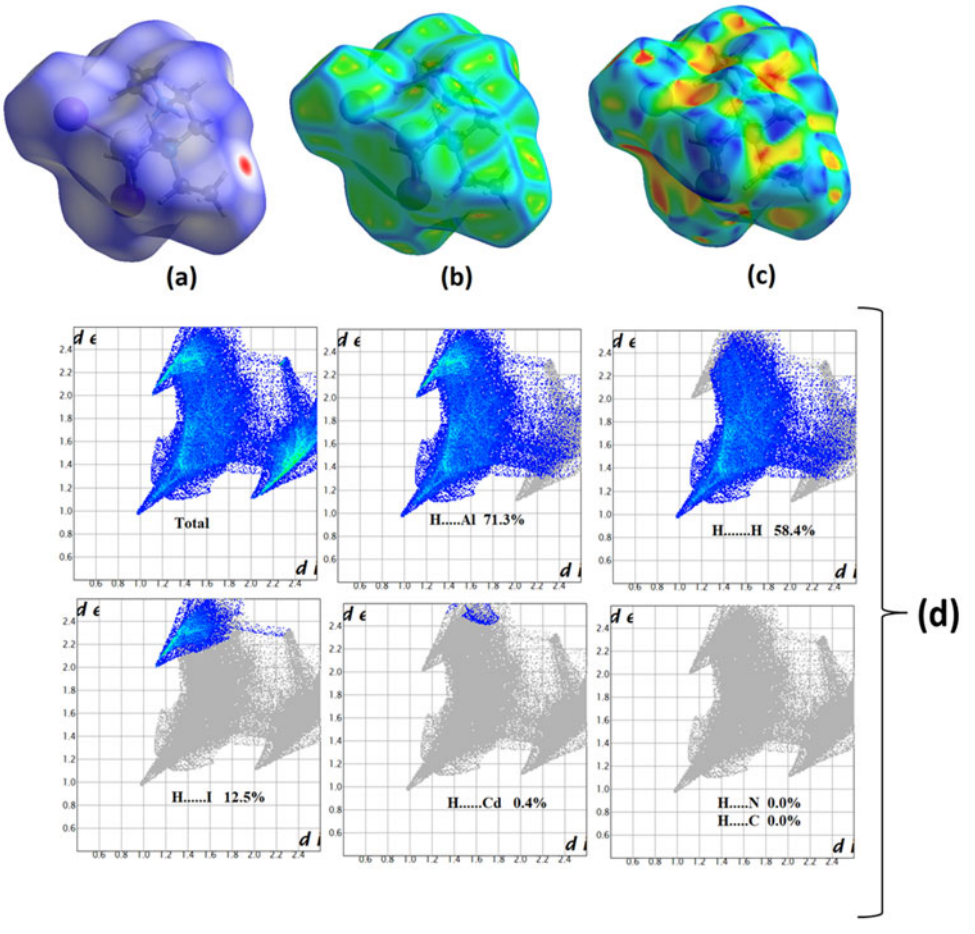

Figure 7. (a) d_{norm}, (b) curvedness, (c) shape index mapped, and (d) inside … outside atom fingerprint ratio for N∩N″ CdI_2.

other atoms are green in between nucleophile/electrophilic sites [26, 27]. Even in the presence of both electrophilic and nucleophilic sites, the iodide nucleophilicity is not strong enough to form an H-bond, which corresponded to the XRD-measurement.

The DFT/B3LYP-Mulliken population charge analyses of **2** are illustrated in Figure 8 and Table 5. In general, the 2I, 2N and all carbons were detected as nucleophilic sites, while the electrophilic sites are Cd and hydrogens, the most electrophilic hydrogens were close to one CH_3 proton (H5) with 0.351924e; the same atom was responsible for H … H supramolecular noncovalent intermolecular interaction in XRD. This value supported the XRD-packing result of having only H … .H supramolecular interaction in the crystal lattice.

3.6. TG/DTG

The TG/DTG of **2** was performed in an open atmosphere at 10 °C/min heating rate. Complex **2** has high thermal stability and decomposed thermally *via* two steps, as

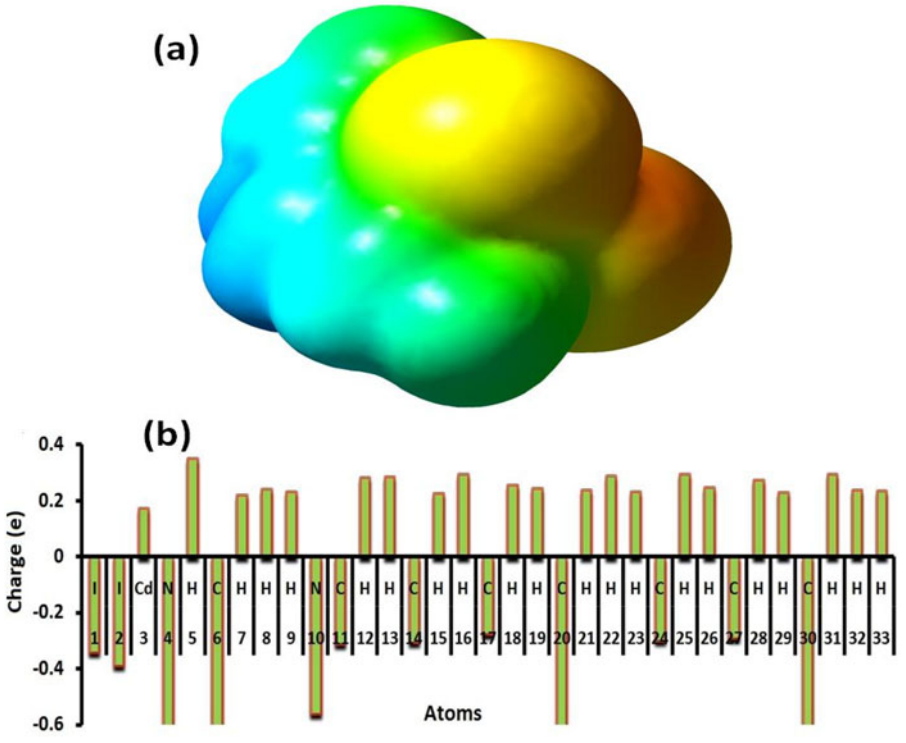

Figure 8. (a) MEP and (b) Mulliken atomic charge for N∩N″CdI_2.

Table 5. Mulliken population charge analysis for N∩N″CdI_2.

Atom No.	Atom	Mull (e)	Atom No.	Atom	Mull (e)
1	I	–0.341822	18	H	0.258511
2	I	–0.387857	19	H	0.246275
3	Cd	0.173789	20	C	–0.676756
4	N	–0.626619	21	H	0.240037
5	H	0.351924	22	H	0.28912
6	C	–0.663428	23	H	0.234095
7	H	0.222784	24	C	–0.299092
8	H	0.241935	25	H	0.294845
9	H	0.233653	26	H	0.247754
10	N	–0.559969	27	C	–0.290087
11	C	–0.312988	28	H	0.276176
12	H	0.285399	29	H	0.232135
13	H	0.287959	30	C	–0.671448
14	C	–0.305931	31	H	0.294573
15	H	0.228795	32	H	0.240641
16	H	0.295531	33	H	0.237315
17	C	–0.277249			

illustrated in Figure 9, decomposing to CdO final product [8, 12, 18]. The first loss started at ∼280 °C, from N1,N1,N2-triethylethane-1,2-diamine ligand pyrolysis (no dehydration), to give CdI_2 from 260 to 320 °C with 28.2% weight lost (27.6% theoretical). In the second step, CdI_2 undergoes a known broad decomposition step, from iodide loss forming oxide from 320 to 430 °C. The remaining residue of 25.2% (25.5% theoretical) is due to CdO final product [18].

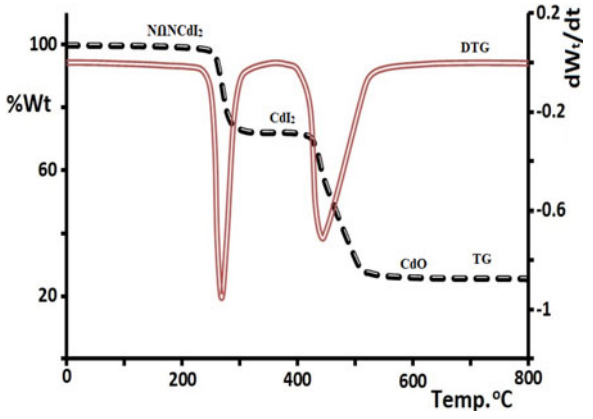

Figure 9. TG-DTG of **2**.

4. Conclusion

Two new tetrahedral complexes, [N∩N″CdX_2], using N1,N1,N2-triethylethane-1,2-diamine as asymmetrical ligand were obtained in good yields. The distorted tetrahedral geometry around cadmium(II) in **2** was confirmed by XRD and computed by DFT. Experimentally, the crystal lattice reflected the presence of H….H noncovalent supramolecular interactions only; these interactions were proven by Hirshfeld surface MEP and Mull analysis. Moreover, MS, FT-IR, UV-vis, EDX, CHN-elemental analyses and ^{1}H-NMR confirmed mononuclear complexes. The computed DFT-structure parameters, MEP, Mull, FMO, TD-SCF, B3LYP-IR, and GRD quantum analysis are consistent with experimental parameters. TG/DTG showed N∩N″CdI_2 complex with stability, decomposing *via* two steps to produce CdO as final product.

Disclosure statement

No potential conflict of interest was reported by the authors.

References

[1] J. Deckert. *Biometals*., **18**, 475 (2005).
[2] W. Lane, A. Saito, N. George, J. Pickering, C. Prince, F. Morel. *Nature*, **42**, 435 (2005).
[3] F. Jalilehv, B.O. Leung, V. Mah. *Inorg. Chem*., **48**, 5758 (2009).
[4] T. Ishihara, E. Kobayashi, Y. Okubo, Y. Suwazono, T. Kido, M. Nishijyo, H. Nakagawa, K. Nogawa. *Toxicology*, **163**, 23 (2001).
[5] M. Hakimi, Z. Mardani, K. Moeini, E. Schuh, F. Mohr. *Z. Naturforsch*., **68**, 267 (2013).
[6] A.S. Aldwayya, F.M. Al-Jekhedab, M. Al-Noaimi, B. Hammouti, T.B. Hadda, M. Suleiman, I. Warad. *Int. J. Electrochem. Sci*., **8**, 10506 (2013).
[7] S. Mondal, A. Dipankar. *J. Mol. Struct*., **1154**, 348 (2018).
[8] I. Warad, A.A. Khan, M. Azam, S.I. Al-Resayes, S.F. Haddad. *J. Mol. Struct*., **1062**, 167 (2014).
[9] Q.-Y. Huang, Z.-B. Zheng, Y.-P. Diao. *J. Mol. Struct*., **1088**, 188 (2015).
[10] A. Prakash, B.K. Singh, N. Bhojak, D. Adhikari. *Acta, Part A*, **76**, 356 (2010).
[11] I. Warad, F. Al-Rimawi, A. Barakat, S. Affouneh, N. Shivalingegowda, N.K. Lokanath, I.M. Abu-Reidah. *Chem. Cent. J*., **10**, 38 (2016).

[12] I. Warad, M. Abdoh, N. Shivalingegowda, N.K. Lokanath, R. Salghi, M. Al-Nuri, S. Jodeh, S. Radi, B. Hammouti. *J. Mol. Struct.*, **1099**, 323 (2015).
[13] M. Montazerozohori, S. Joohari, S. Musavi. *Spectrochim. Acta, Part A*, **73**, 231 (2009).
[14] I. Warad, M. Azam, S.I. Al-Resayes, M.S. Khan, P. Ahmad, M. Al-Nuri, S. Jodeh, A. Husein, S.F. Haddad, B. Hammouti, M. Al-Noaimi. *Inorg. Chem. Commun.*, **43**, 155 (2014).
[15] A. Banerjee, P. Maiti, T. Chattopadhyay, K. Banu, M. Ghosh, E. Suresh, E. Zangrando, D. Das. *Polyhedron*, **29**, 951 (2010).
[16] S. Banerjee, A. Bauzá, A. Frontera, A. Saha. *RSC Adv.*, **6**, 39376 (2016).
[17] B. Song, H. Wei, Z. Wang, X. Zhang, M. Smet, W. Dehaen. *Adv. Mater.*, **19**, 416 (2007).
[18] G.M. Sheldrick. *Acta Crystallogr. A Found. Crystallogr.*, **64**, 112 (2008).
[19] M.J. Frisch, G.W. Trucks, H.B. Schlegel, G.E. Scuseria, M.A. Robb, J.R. Cheeseman, G. Scalmani, V. Barone, B. Mennucci, G.A. Petersson, H. Nakatsuji. *GAUSSIAN09*, Gaussian Inc., Wallingford, CT, USA (2009).
[20] S.K. Wolff, D.J. Grimwood, J.J. McKinnon, D. Jayatilaka, M.A. Spackman. *Crystal Explorer 2.1.*, University of Western Australia, Perth (2007).
[21] I. Alkorta, J. Elguero, S.J. Grabowski. *J. Phys. Chem. A*, **112**, 2721 (2008).
[22] M.R. Aouad, M. Messali, N. Rezki, N. Al-Zaqri, I. Warad. *J. Mol. Liq.*, **264**, 621 (2018).
[23] M.A. Spackman, J.J. McKinnon. *Cryst. Eng. Comm.*, **4**, 378 (2002).
[24] M.A. Spackman, D. Jayatilaka. *Cryst. Eng. Comm.*, **11**, 19 (2009).
[25] D.C. Onwudiwe, P.A. Ajibade. *Int. J. Mol. Sci.*, **13**, 9502 (2012).
[26] M.R. Aouad, M. Messali, N. Rezki, M.A. Said, D. Lentz, L. Zubaydi, I. Warad. *J. Mol. Struct.*, **11180**, 455 (2019).
[27] M. Altowyan, A. Barakat, A. Al-Majid, H. Ghabbour, Z. Zarrouk, I. Warad. *BMC Chem.*, **13**, 11(2019).